Resilient Wide-Area Damping Control Using GrHDP to Tolerate Communication Failures

Yu Shen, *Student Member, IEEE*, Wei Yao, *Senior Member, IEEE*, Jinyu Wen, *Member, IEEE*, Haibo He, *Fellow, IEEE*, Lin Jiang, *Member, IEEE*

***Abstract*—This paper proposes a goal representation heuristic dynamic programming (GrHDP) based resilient wide-area damping controller (WADC) for voltage source converter high voltage direct current (VSC-HVDC) employing redundant wide-area signals as input signals to tolerate communication failure. A supervisory fuzzy logic module (FLM) is proposed and added in the resilient WADC to adjust the learning rate of GrHDP online when encountering communication failure. Moreover, the resilient WADC does not need the accurate model of the power system and has the adaptability to the variation of operation conditions and communication failures. Case studies are conducted in a 10-machine 39-bus system with one VSC-HVDC transmission line. Simulation results show that the resilient WADC can counteract the negative impact of communication failures on control performance under a wide range of system operating conditions.**

***Index Terms*—Interarea oscillation, wide-area damping control, communication failure, goal representation heuristic dynamic programming, fuzzy logic.**

NOMENCLATURE

$\boldsymbol{X(t)}$ system feedback signals.
$\Delta P_{\text{mod}}(t)$ modulation signal for VSC-HVDC.
$E_a(t)$ error of action network.
$E_c(t)$ error of critic network.
$E_r(t)$ error of goal network.
$J(t)$ cost function of GrHDP.
$J^*[\boldsymbol{X(t)}]$ minimized cost function.
$l(t)$ learning rate.
$N_a(t)$ maximum iteration number of action network.
$N_c(t)$ maximum iteration number of critic network.
$N_r(t)$ maximum iteration number of goal network.
$r(t)$,$r[\boldsymbol{X(t)},u(t)]$ external reward signal.
$S(t)$ internal reward signal.
$u(t)$ control action.
$U[\boldsymbol{X(t)},u(t),t]$ utility function.
$U_c(t)$ desired ultimate target.
$W_a(t)$ weights of action network.
$W_c(t)$ weights of critic network.
$W_r(t)$ weights of goal network.

Manuscript received July 3, 2017; revised December 4, 2017; accepted February 3, 2018. This work was supported in part by National Natural Science Foundation of China under Grant 51529701 and Grant 5157707 and in part by the National Basic Research Program of China (973 Program) under Grant 2014CB247400. Paper no. TSG-00921-2017 *(Corresponding author: Wei Yao.)*

Y. Shen, W. Yao, and J. Y. Wen are with State Key Laboratory of Advanced Electromagnetic Engineering and Technology, School of Electrical and Electronic Engineering, Huazhong University of Science and Technology, Wuhan, 430074, China. (email: yshen@hust.edu.cn; w.yao@hust.edu.cn; jinyu.wen@hust.edu.cn)

H. B. He is with the Department of Electrical, Computer and Biomedical Engineering, University of Rhode Island, Kingston, RI 02881, USA (email: he@ele.uri.edu).

L. Jiang is with the Department of Electrical Engineering & Electronics, University of Liverpool, Liverpool L69 3GJ, U.K. (e-mail: ljiang@liverpool.ac.uk)

I. INTRODUCTION

Interarea oscillation is one of the challenges for the stable and secure operation of an interconnected power system [1]–[4]. The effectiveness in damping interarea oscillations of wide-area damping controller (WADC) using remote signal obtained from wide-area measurement system (WAMS) has been proved in [5]–[8]. However, wide-area signals need to be transmitted via a fast and reliable communication system. Although existing techniques ensure the reliability of communication system in a certain degree, there is still possibility of communication failures due to accidental or malicious disruption, which may deteriorate the damping performance of WADC or even destabilize power systems [9].

To prevent the WADC becoming invalid when a wide-area signal is lost due to communication failures, two kinds of measures are proposed. One is that both local and wide-area signals are used as input signals of WADC in [9], [10]. A H_∞ based two-input single-output controller with two degrees of freedom is proposed in [9] and the WADC with only local signal remained is designed by the simultaneous pole-placement method in [10]. However, the damping performance of WADC will be deteriorated as only local signal is available during the communication failures. The other is that multiple redundancy wide-area signals or actuators are employed to ensure system resiliency of communication failures [11], [12]. For example, redundant communication paths are employed in [11], and mathematical morphology identification is used to detect communication failure and then the channel switches automatically from faulty wide-area signal to the backup signals. However, this method needs detection technique to capture significant changes in the transited signal while ignoring minor changes, which is complicated and its accuracy affects the control performance significantly.

For the WADC under network imperfections, a few references have addressed this issue from different aspects [12]–[15]. In [13], Q-learning based control algorithm is employed to obtain the optimal control under both physical and cyber uncertainties. The linear quadratic Gaussian (LQG) based WADC is proposed to deal with the problem of imperfect communication medium in [14]. A fault tolerant controller is proposed for power system to handle sensor failure in [15]. In addition, actuator redundancy is used to achieve higher reliability in [12]. When an actuator fails due to loss of communication, the WADC control signals are re-routed to other available actuators without redesigning the nominal WADC. However, most of these WADCs are designed based on the mathematic model of power system, which is difficult to obtained for a practical power system.

Regarding model-free designing methods which only need measured input/output signals of the controlled system, adaptive dynamic programming (ADP) gains much popularity for the ADP based controller achieves optimal control action by solving the Bellman's optimal equation [16]–[19]. Ref. [20] proposes the goal representation heuristic dynamic programming (GrHDP), which is one of the members in the ADP family but the new structure makes GrHDP have stronger learning ability and adaptivity [21]. As a model-free designing methods, the GrHDP algorithm has strong self-adaptivity to the variation of the system operating conditions and parameter uncertainties through updating the weighting parameters online based on the input/output signals of the system. The effectiveness of applying GrHDP in the field of stability control of wind farm, excitation control of generators and the control of flexible AC transmission system have been proved in [22]–[24]. Ref. [25] verifies the GrHDP based WADC with adaptive delay compensator can compensate the time-varying delays effectively under a wide-range of system operating conditions [26].

In this paper, a GrHDP algorithm based resilient WADC using three wide-area input signals is proposed to improve the resiliency of power system. Multiple communication paths can guarantee that there is at least one input signal remained in most cases. A supervisory fuzzy logic module (FLM) is also used in resilient WADC to adjust the learning rate of GrHDP under communication failure, which can accelerate the online learning of GrHDP. Consequently, encountering communication failures, the resilient WADC still maintains a good control performance with the rest wide-area signals depending on its strong online learning ability and adaptability. Considering that voltage source converter high voltage direct current (VSC-HVDC) has flexible and large regulation ability, VSC-HVDC can be a suitable and effective actuator of damping interarea oscillation of a power system [27], [28]. Since the ability of the GrHDP based WADCs to compensate time delays and adapt to the change of system operating conditions have been fully investigated and verified in [29], [30], this paper mainly focuses on designing the resilient WADC for VSC-HVDC to suppress interarea oscillation in an AC/DC power system to tolerate communication failure.

This paper extends the work reported in [30] and its main contributions are summarized as follows:

- This paper concerns the design of the GrHDP based resilient WADC to tolerate communication failure, while [30] mainly focuses on design an adaptive supplementary damping controller to adapt to the change of the system operating condition without considering the impact of communication network.
- Based on the adaptive controller proposed in [30], this paper proposes a resilient WADC for VSC-HVDC by employing redundant wide-area signals as input signals to tolerate communication failure. Moreover, a supervisory fuzzy logic module (FLM) is proposed and added in the resilient WADC to adjust the learning rate of GrHDP online when encountering communication failure.
- The effectiveness of the proposed resilient WADC are verified under both different communication failure scenarios and operating conditions, while the adaptive supplementary damping controller proposed in [30] is only verified under different operation conditions.

The rest of this paper is organized as follows. Section II introduces the control system of VSC-HVDC. Section III describes the proposed resilient WADC, including GrHDP, FLM, and the training process of resilient WADC. In Section IV, both resilient and conventional WADCs are designed for VSC-HVDC in a New England 10-machine 39-bus power system with one VSC-HVDC transmission lines. Section V conducts a case study to verify the effectiveness of the resilient WADC. Finally, conclusions are drawn in Section VI.

II. Control System of VSC-HVDC

In this paper, the GrHDP based resilient WADC is designed and added into the control system of VSC-HVDC. Therefore, the control system of VSC-HVDC is briefly introduced in this section. Fig. 1 shows the structure of the control system of VSC-HVDC. It can control the active and reactive power transmitted in DC transmission lines, respectively, and also can control the DC voltage and AC voltage. P_{ref}, Q_{ref}, $V_{\mathrm{ac\_ref}}$ and $V_{\mathrm{dc\_ref}}$ are reference instructions generated by the system-level control of VSC-HVDC. According to the reference instructions, the outer-loop power control generates inner d-q axis current reference signals $i_{\mathrm{d1}}^{\mathrm{ref}}$, $i_{\mathrm{q1}}^{\mathrm{ref}}$, $i_{\mathrm{d2}}^{\mathrm{ref}}$, and $i_{\mathrm{q2}}^{\mathrm{ref}}$. According to these reference signals, inner current control generates the current instructions, and finally firings are generated to control the valves of converter stations by valve-level control of VSC-HVDC. Moreover, the inner current control employs the d-q axis decouple control structure, which makes VSC-HVDC have the ability of active power and reactive power decoupled control and flexible regulation capacity. ΔP_{mod}, ΔQ_{mod}, $\Delta V_{\mathrm{dc\_mod}}$ and $\Delta V_{\mathrm{ac\_mod}}$ can all be added in the control loop as modulate signals to improve the dynamic characteristic of AC/DC power system. The detailed model of VSC-HVDC can be found in [31].

In this paper, active power modulation is employed. According to the system feedback signals, the resilient WADC (RWADC) generates a modulation signal ΔP_{mod} which is added to P_{ref} as an additional reference signal to modulate the active power transmitted in DC transmission line to damp the interarea oscillations in an AC/DC power system.

III. GrHDP based Resilient WADC

The structure of the GrHDP based resilient WADC for VSC-HVDC is shown in Fig. 2. It can be found that the resilient WADC employs three wide-area feedback signals as the input signals. When the active power deviation changes,

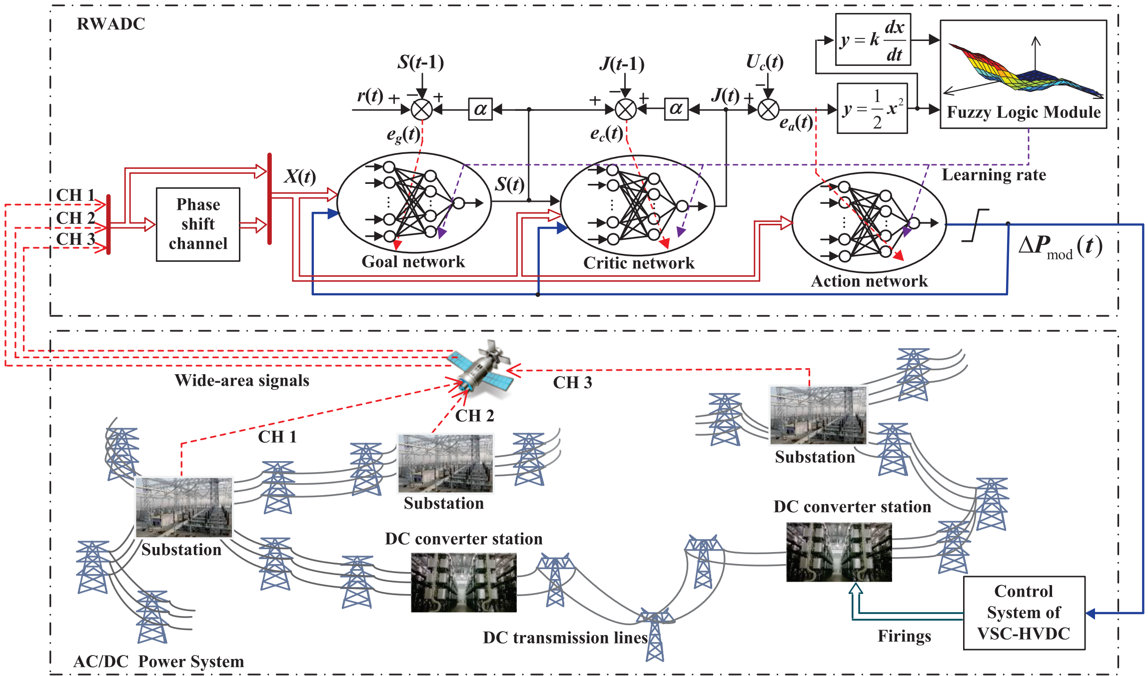

Fig. 2. The structure of RWADC of VSC-HVDC for AC/DC power system.

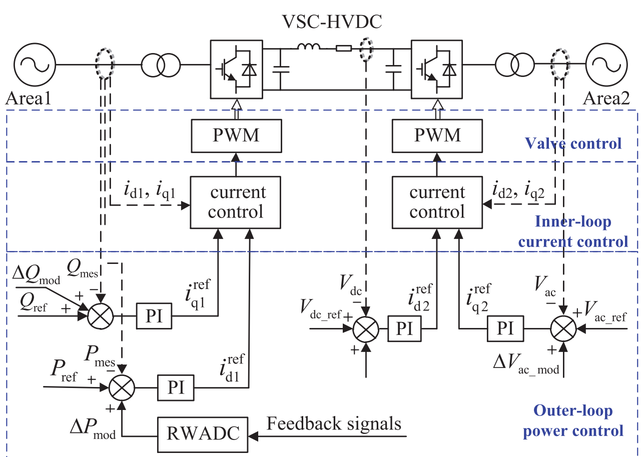

Fig. 1. The control system of VSC-HVDC.

the proposed resilient WADC is triggered and the weights of each network of GrHDP will be updated online to make the controller achieve an optimal control action. The output signal of resilient WADC is a modulation signal $\Delta P_{\mathrm{mod}}(t)$ for the control system of VSC-HVDC, which can modulate the active power transmitted in DC lines. Since the GrHDP based resilient (WADC) is a model-free method which only needs measured input and output signals of the controlled system, it has the advantages of quick online learning ability and strong adaptivity. Moreover, the learning rate of GrHDP can be adjusted online to ensure the damping performance under communication failures.

A. Introduction of GrHDP

Fig. 2 also shows the three-neural-network structure of GrHDP, which consists of the goal network, critic network and action network. The goal network is newly developed by GrHDP based on the two-neural-network structure of HDP.

1) Output of each network: The newly developed goal network of GrHDP generates an adaptive internal reward signal $S(t)$, which can facilitate the mapping relationship between the control action and the system state. Internal reward signal $S(t)$ is generated to replace the external reward signal $r(t)$, which is a fixed value or fixed function related to the power system states. Critic network generates the cost function $J(t)$, which should be minimized during the control process. According to the three feedback signals of the power system, action network generates the control instruction $\Delta P_{\mathrm{mod}}(t)$ to the control system of VSC-HVDC, which can regulate the active power in DC transmission lines and dampen the interarea oscillations of AC power system.

2) Target of GrHDP: Since GrHDP is one of the members in the adaptive dynamic programming (ADP) family, the ultimate target for GrHDP is also to solve the Bellman's optimal equation [20]:

$$J[\boldsymbol{X(i)}, i] = \sum_{t=i}^{\infty} \alpha^{t-i} U[\boldsymbol{X(t)}, u(t), t] \tag{1}$$

where, U is the utility function and α is a discount factor. $\boldsymbol{X(t)}$ and $u(t)$ are the input and output signal of action network, respectively.

In order to minimize the cost function $J(t)$, an optimal control action should be found, which is shown in Eq. (2).

$$J^*[\boldsymbol{X(t)}] = \min_{u(t)} \{ r[\boldsymbol{X(t)}, u(t)] + \alpha J^*[\boldsymbol{X(t+1)}] \} \tag{2}$$

where $r[\boldsymbol{X(t)}, u(t)]$ is the utility function in equation (1) and namely, the reward function of each time step. $\boldsymbol{X(t)}$ is the vector related with the system feedback signals in this paper and $u(t)$ is the control signal $\Delta P_{\mathrm{mod}}(t)$.

3) Weights updating of GrHDP: To generate an optimal control action, the weights of three neural networks are updated during the control process. Since these three networks are all multilayer feed forward neural networks, their weights are updated by back propagation rules [20].

The error of critic network, goal representation network and action network are defined as follows:

$$\begin{aligned} e_c(t) &= \alpha J(t) - [J(t-1) - S(t)]; \quad & E_c(t) &= \frac{1}{2}e_c(t)^2 \\ e_r(t) &= \alpha S(t) - [S(t-1) - r(t)]; \quad & E_r(t) &= \frac{1}{2}e_r(t)^2 \\ e_a(t) &= J(t) - U_c(t); \quad & E_a(t) &= \frac{1}{2}e_a(t)^2 \end{aligned} \tag{3}$$

where the $J(t-1)$ and $S(t-1)$ are the history signal one time step ago, U_c is the desired ultimate target of GrHDP, which is set to be zero to minimize $J(t)$. The gradient descent method is adopted to solve this optimization.

The weights of neural network are updated by rules:

$$\begin{aligned} \Delta W_{ij}^{(1)}(t) &= -l(t)\frac{\partial E(t)}{\partial W_{ij}^{(1)}(t)} \\ \Delta W_{i}^{(2)}(t) &= -l(t)\frac{\partial E(t)}{\partial W_{i}^{(2)}(t)} \end{aligned} \tag{4}$$

where $l(t)$ is the learning rate of neural network, $W_{ij}^{(1)}$ and $W_i^{(2)}$ denote the weights of the input to hidden layer and the hidden to output layer of the neural network, respectively.

B. Introduction of FLM

Fuzzy logic module is adopted to regulate the learning rate of each network of GrHDP under communication failures. For example, if two wide-area signals are lost due to communication failures, the value of $J(t)$ will decrease significantly, and the error E_a will also decrease significantly, which makes the adjustment values of weights become very small and reduces the regulation ability of GrHDP. The desired situation is that GrHDP can generate a great weights adjustment after communication failures to maintain the control performance with the remaining signal. To achieve this goal, the learning rate of the neural network of GrHDP is changed by FLM under communication failures.

It can be found from Fig. 2 that the input variables of FLM are E_a and its derivative $k*dE_a/dt$, of which the factor k is used to keep them within the same range. The output variable of FLM is the learning rate $l(t)$ of GrHDP. Each variable has its own membership function. The fuzzy rules are set to increase the learning rate when communication failures occur and keep a suitable learning rate under normal operation conditions.

C. Training of RWADC

To achieve a good control performance, the three networks of RWADC need pre-training to achieve appropriate weights. The pre-training process should be conducted under various operation conditions and disturbances. At every time step, the three networks of GrHDP conduct the weights updating and the learning rate is determined by FLM one time step earlier. Take the pre-training process at t step as an example, the training and learning step is shown in Fig. 3.

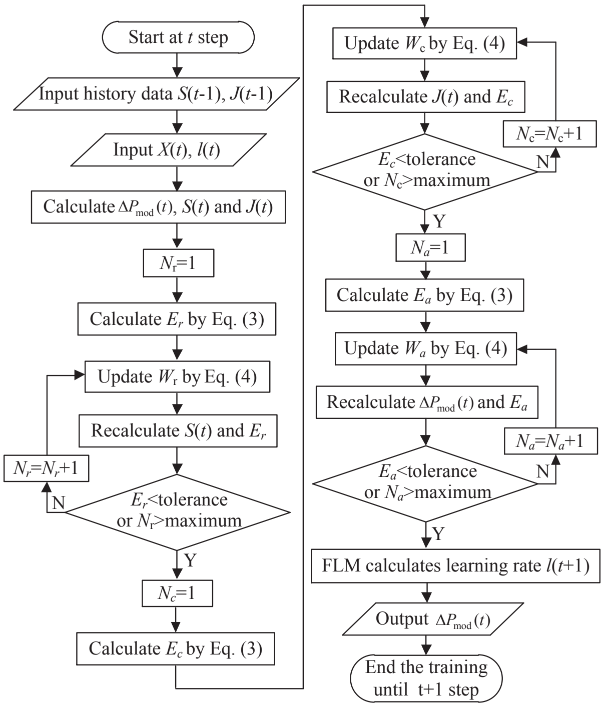

Fig. 3. The training and learning process at t step.

The detailed process is described as follows:

- According to the input signal $X(t)$, initial output of each network are calculated respectively, such as the external reward signal $r(t)$, control action $\Delta P_{\text{mod}}(t)$ and internal reward signal $S(t)$.
- The error of goal representation network $E_r(t)$ is calculated according to $r(t)$, $S(t)$, and the history data $S(t-1)$, then the weights of goal representation network are tuned according to equation (4) until the stop criterion is satisfied, and finally a new internal reward signal $S(t)$ is generated.
- The error of critic network $E_c(t)$ is calculated, the weights are updated until the stop criterion is satisfied, and a new cost value $J(t)$ is generated.
- The error of action network $E_a(t)$ is calculated, the weights are updated until the stop criterion is satisfied. After weights updating, the action network generates a new control action $\Delta P_{\text{mod}}(t)$. Compared to the $\Delta P_{\text{mod}}(t)$ in the first step, $\Delta P_{\text{mod}}(t)$ here is updated and the control performance is improved.
- Once the weights of three networks are tuned, they are fixed after that and FLM calculates the learning rate for the next time step. The training process repeats from the first step when entering the $t+1$ time step.

Once the training process is finished, the updated weights are employed as initial weights of the three networks of RWADC. Moreover, RWADC has the ability of online learning. In other words, if the operation condition of the power system varies or severe disturbance occurs, weights of the three

TABLE I
MODAL ANALYSIS RESULTS OF THE BENCHMARK

Mode No.	Mode Type	Damping Ratio ξ	Freq. f (Hz)	Mode Shape
1	Inter-area	0.0162	0.6721	10 v.s. (4,5,6,7,9)
2	Inter-area	0.0465	0.9862	5 v.s. 9
3	Inter-area	0.1341	1.0790	(2,3) v.s. 9

networks can be updated online and the updating process is the same as above from the first step to the fourth step.

IV. CONTROLLER DESIGN

A. Benchmark Description

The AC/DC power system modeling is discussed in this section. Fig. 4 presents the structure of the benchmark based on a New England 10-machine 39-bus system. The difference is that one VSC-HVDC transmission line is located between bus 16 and bus 17, with 100 MW DC transmission power. The detailed parameters of the system are given in [33], [34]. Note that some modifications have been made to show the weak mode so that the controller design procedure can be illustrated more clearly. Generators G1, G2, G3, G8 and G9 are equipped with a power system stabilizer to enhance the damping ratio of the local modes. In addition, the impact of the governor system has been ignored.

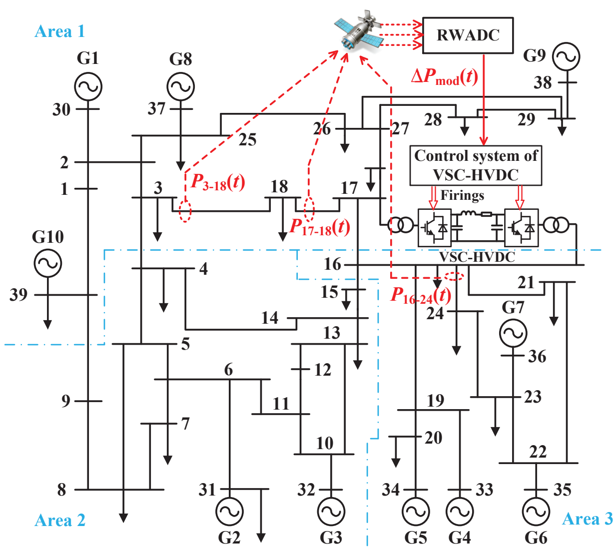

Fig. 4. The structure of benchmark system

Under the initial operation condition, modal analysis is conducted and the results are shown in Table I. As listed in Table I, there exist three interarea oscillation modes and the damping ratio of mode 1 is less than 3%, so it is necessary to design a damping controller for this weak mode.

B. Design of Resilient WADC

The theory of modal observability has been used to select suitable feedback signals for resilient WADC. It can be found that the active power of transmission line P_{3-18}, P_{17-18} and P_{16-24} all have high observability for mode 1 and thus they are chosen as the input signals of the resilient WADC [33].

1) Design of GrHDP: For the design of GrHDP, if only ΔP_{3-18}, ΔP_{17-18} and ΔP_{16-24} are chosen as input signals, the multilayer feed forward neural networks of GrHDP are unable to realize the desired phase change. To solve the problem, by shifting the phase of each input signal via a parallel phase shift channel, additional phase shifted input signals are generated [30]. The phase shift channel of GrHDP is shown in Fig.5. k_{NF1} to k_{NF6} are normalization coefficients to keep the original signal and its phase shifted signal in the same numeric range. In this paper, $k_{\mathrm{NF1}} = k_{\mathrm{NF3}} = k_{\mathrm{NF5}} = 0.27$, $k_{\mathrm{NF2}} = k_{\mathrm{NF4}} = k_{\mathrm{NF6}} = 0.063$. T_{m1} to T_{m3} are time constant, $T_{\mathrm{m1}} = T_{\mathrm{m2}} = T_{\mathrm{m3}} = 0.05$. The parameters of GrHDP are listed in Table II.

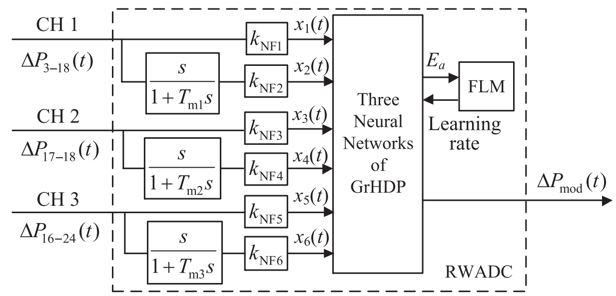

Fig. 5. Phase shift channels of RWADC.

TABLE II
THE PARAMETERS OF GRHDP

Neural Network	Action	Critic	Goal
Number of input layer	6	8	7
Number of output layer	1	1	1
Number of hidden layer	3	3	3
Learning rate	0.018	0.018	0.018
Maximum iteration number	30	50	50
Margin of error	1e-8	1e-8	1e-8
Range of weight	±10	±10	±10

The external reward signal $r(t)$ is defined as:

$$r(t) = -\frac{1}{6}\sum_{i=1}^{6} x_i(t)^2 \tag{5}$$

2) Design of FLM: The input variables are the error of action network E_a and its differential dE_a/dt. Fig. 6 shows the control block diagram of the proposed FLM. Saturation elements are used to simplify the fuzzy rules of FLM. E_a is limited between 0 and 0.1, and dE_a/dt is limited between -0.1 and 0.1.

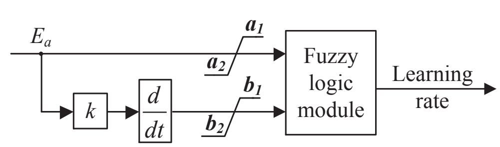

Fig. 6. Fuzzy logic module of RWADC.

Fig. 7 shows the membership function of input and output variables. In this paper, the fuzzy membership functions of input variables are selected in the form of Gauss function. The fuzzy membership function of output variable is in triangle form. Three linguistic variables for E_a are used, which are L (Low), M (Medium), and H (High). Three linguistic variables for dE_a/dt are used, which are N (Negative), Z (Zero), and P (Positive). There are also three linguistic variables for output variable, namely, LW (low), MD (medium) and HG (high).

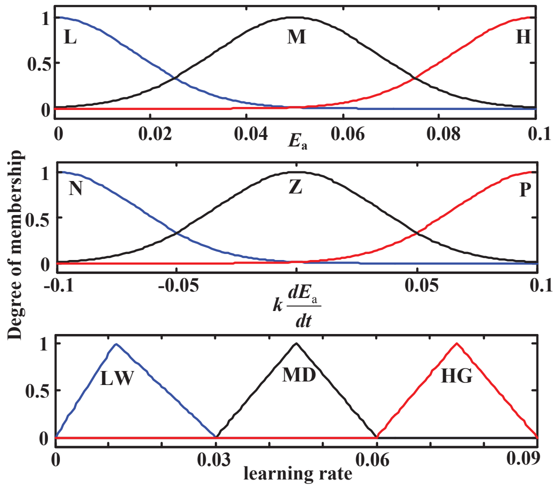

Fig. 7. Membership function of input and output variables

With two input variables, the fuzzy rules are given as follows:

$$If\ (E_a = A_i)\ \ and\ \ (k\frac{dE_a}{dt} = B_i),\ \ then\ (l = C_i) \tag{6}$$

where A_i and B_i are the fuzzy sets, C_i is the designed output parameters and i is the number of membership functions of each input.

Fig. 8 is the output surface of FLM. It can be found that the learning rate can be determined by the two input signals.

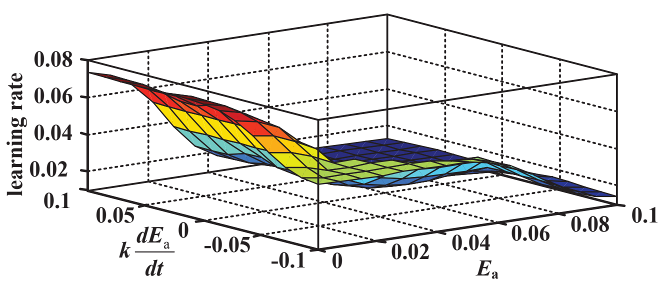

Fig. 8. Output surface of FLM

The fuzzy rule-based matrix is listed in Table III.

TABLE III
THE FUZZY RULE-BASED MATRIX

kdE_a/dt \ E_a	L	M	H
N	MD	MD	LW
Z	HG	LW	LW
P	HG	LW	LW

Furthermore, to maintain a normal learning rate without communication failure or return to the normal learning rate when RWADC has worked for a period, a judgment element related to $r(t)$ is employed. That is, if $|r(t)| < 0.001$ and $|\int r(t)dt| < 0.01$, FLM is put into operation, otherwise it is out of service.

C. Design of Conventional WADC

In this paper, a conventional WADC (CWADC) is designed for comparison. The CWADC consists of two lead-lag elements and employs only one wide-area input signal. Since CWADC is a single-input-single-output controller, it cannot work if the only input signal is lost under communication failure.

The parameters of CWADC are designed based on the residue method and the linearization model of the benchmark under a special operation condition. The input signal of CWADC is P_{3-18} and the transfer function is:

$$G_{\mathrm{CWADC}}(s) = \frac{\Delta P_{\mathrm{mod}}(t)}{\Delta P_{3-18}(t)} = 0.06(\frac{1+0.7144s}{1+0.0785s})^2 \tag{7}$$

With the designed CWADC, the damping ratio of the interarea mode 1 increases from 1.62% to 8.01%. Meanwhile, the damping ratio of interarea mode 2 decreases from 4.65% to 3.97%, mode 3 slightly increases from 13.41% to 13.7%.

D. Design of Robust WADC

In addition, the robust WADC proposed in [35] is also designed for comparison. The original 84th order linearized model of the power system is reduced to a 11th-order model by the balanced model reduction method. Then the *hinfmix* function provided in the LMI Control Toolbox of Matlab is used for control synthesis [36], [37]. Weighting functions are given by

$$W_1 = \frac{100}{10s+1},\quad W_2 = 1e-5,\quad W_3 = \frac{30}{10s+100} \tag{8}$$

By using the balanced model reduction method to reduce the order of the obtained controller, the transfer functions of the designed robust WADC is as follows.

$$G_{\mathrm{robust\ WADC}}(s) = \frac{10s^2+35.34s+28.19}{s^3+0.489s^2+0.707s+0.07} \tag{9}$$

V. SIMULATION VERIFICATION

To verify the effectiveness of the proposed resilient WADC, different scenarios are conducted in this section, such as without communication failure, with one channel communication failure, and with two channel communication failures. Moreover, the effectiveness of the FLM and robustness of the resilient WADC to variation of operating condition and time delay are also verified.

A. Without Communication Failure

In the initial operation conditions, there is approximately 147 MW and 100 MW active power transmitted in AC and DC transmission line from bus 16 to bus 17.

A single three-phase-ground fault is applied on the line 14-15 near bus 14 at $t = 1$ s, followed by switching off the faulty transmission line 14-15 at $t = 1.1$ s. Without communication failure, Fig. 9 shows the active power response of line 3-18, line 17-18, and line 16-24.

It can also be found that in Fig. 9, without WADC, the oscillation is sustained and the power system cannot maintain stability. With the CWADC, robust WADC, and RWADC, the interarea oscillations can be suppressed quickly within 10 s and the power system maintains the stability. The performance of the robust WADC is better than that of the CWADC. Moreover, due to the ability of online learning, the damping performance of RWADC is better than that of the CWADC and robust WADC.

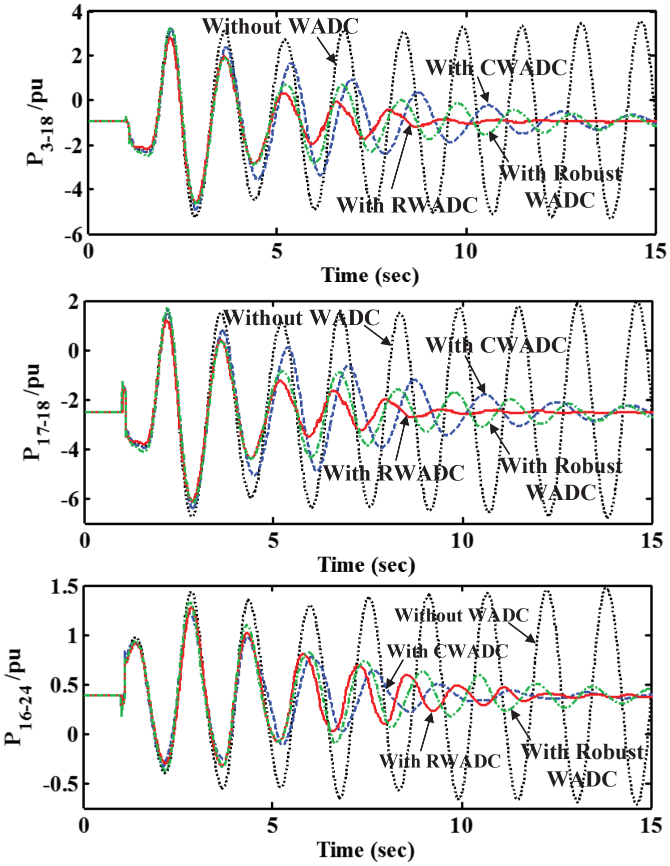

Fig. 9. The response of three wide-area feedback signals P_{3-18}, P_{17-18}, P_{16-24} (without communication failure).

B. With One Channel Communication Failure

To verify the effectiveness of the RWADC under communication failures, one channel communication failure is conducted firstly. Persistent communication failure of one channel is set at 2 s which is 1 s later than the short circuit fault time. The circuit fault is the same as that stated above. Every communication channel is set to be out of service in turn in the simulation. Fig. 10 shows the active power response of transmission lines with one channel communication failure. It can be concluded that any of the three communication channel fails, the RWADC can always achieve a similar damping performance as that without communication failure. The reason is that the magnitude of these output control actions are similar, as is shown in Fig. 10. With three signals as input, it can be found that the loss of one input signal does not have much effect.

C. With Two Channel Communication Failures

Furthermore, two channel communication failures are also tested. At $t = 1s$, a same short circuit fault occurs. At $t = 2$ s, any two channels are out of service because of communication failure. Fig. 11 shows the active power response of transmission lines with two channel communication failures. It can be found that any two of the three channels communication failures occur, the RWADC can always achieve good damping performance. The reason is that RWADC has

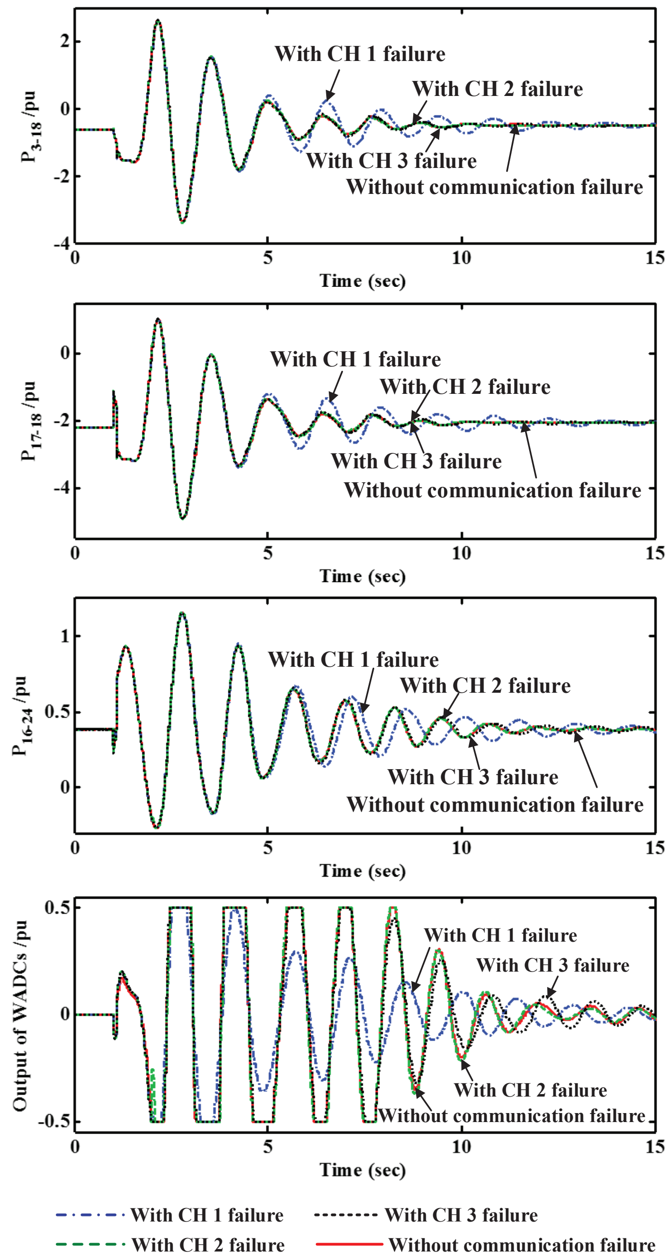

Fig. 10. The response of three wide-area feedback signals P_{3-18}, P_{17-18}, P_{16-24} and the output of RWADC (with one channel communication failure).

the ability of online learning and weights adaptive regulation. With the online learning ability, the control action increased gradually, and finally it achieved a good damping performance. Therefore, when any two of the three channels communication failures occur, the RWADC can always achieve good damping performance.

D. Effectiveness of FLM

In order to observe the effect of FLM, Fig. 12 shows the active power response of transmission lines with or without FLM when encountering the communication failure of channel 1 and channel 2. As shown in Fig. 12, encountering communication failure of channel 1 and channel 2, without FLM, the oscillation attenuates much slower, the damping performance

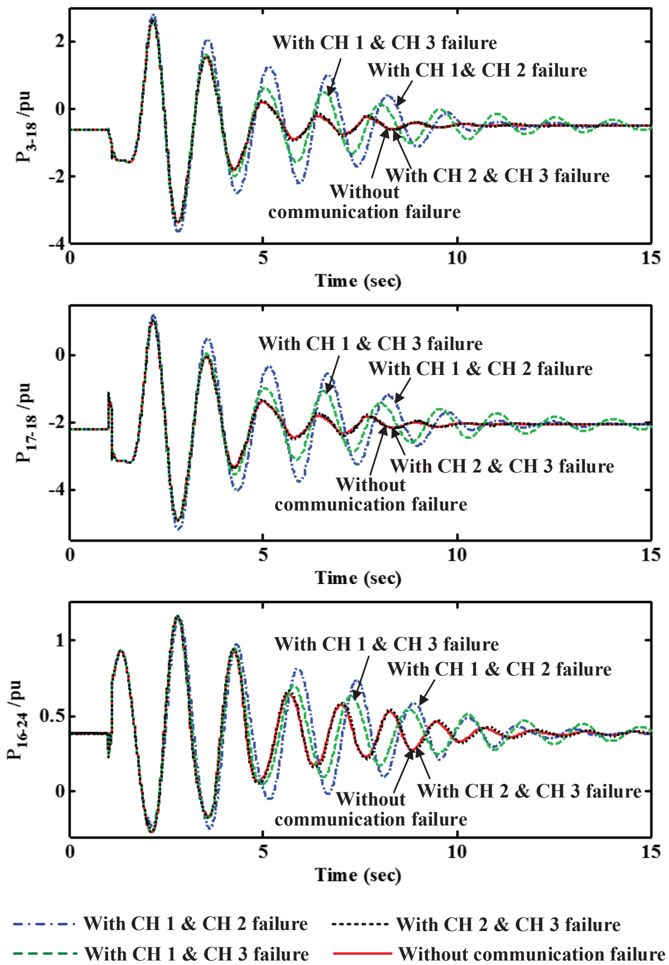

Fig. 11. The response of three wide-area feedback signals P_{3-18}, P_{17-18}, P_{16-24} and the output of RWADC (with two channel communication failures).

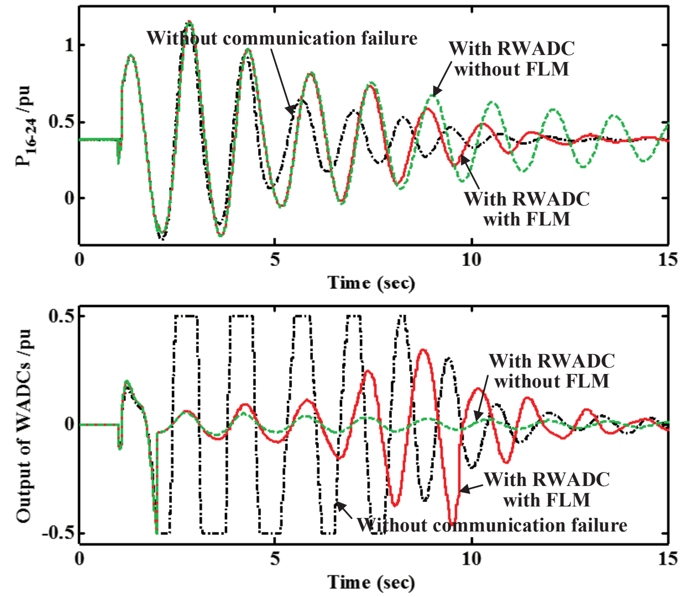

Fig. 12. The response of the remaining wide-area feedback signal P_{16-24} with communication failures of P_{17-18} and P_{16-24} and the output of RWADC (transmission line 14-15 outage happened at 1 s and two channel communication failures happened at 2 s).

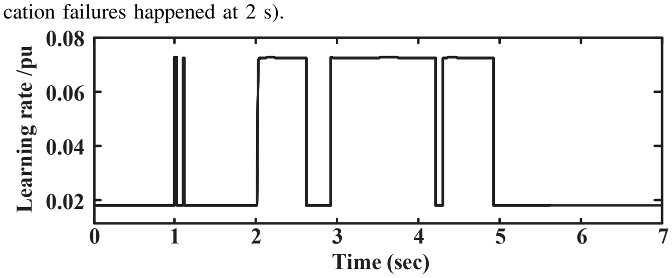

Fig. 13. The learning rate of the three networks of RWADC with FLM (transmission line 14-15 outage happened at 1 s and two channel communication failures happened at 2 s).

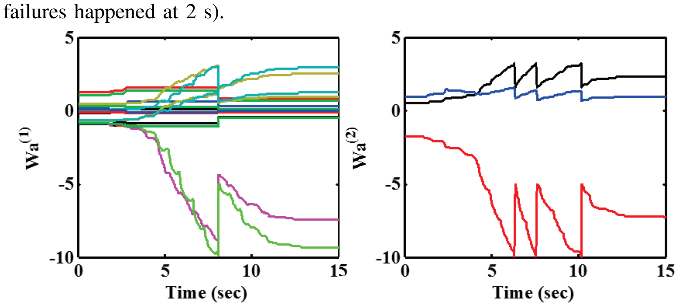

(a) Weights updating of action network with FLM.

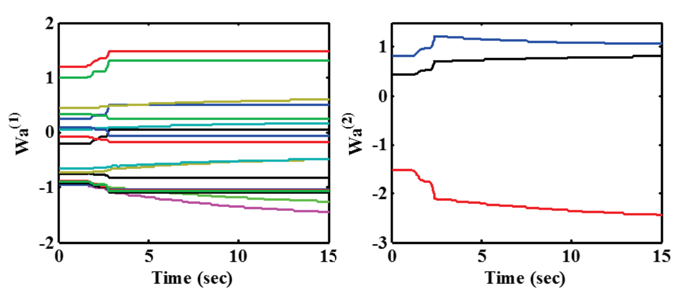

(b) Weights updating of action network without FLM.

Fig. 14. Weights updating of action network with and without FLM.

of RWADC gets worse. However, the RWADC with FLM suppresses the oscillations quickly and the damping performance of RWADC is significantly improved than RWADC without FLM, which verifies the effectiveness of the FLM.

Furthermore, the learning rate of the three networks of RWADC with FLM is shown in Fig. 13. It can be found that the learning rate increases a lot during the first 5 seconds, which increases the weights updating rate and helps to improve the control action. The weights of RWADC with or without FLM are shown in Fig. 14. Comparing Fig. 14(a) with Fig. 14(b), it can be found that the weights updating is accelerated by FLM, for the weights change in a small range without FLM but with FLM the weights change significantly and even achieve the limits. The control performance shown in Fig. 12 verifies the effectiveness of the weights updating in Fig. 14(a).

E. Variation of Operation Condition

In this heavy operation condition, the active power of generator 2 increases from 5.73pu to 7pu, generator 3 increases from 6.5pu to 7pu, generator 4 increases from 6.32pu to 7pu and generator 9 increases from 8.3pu to 10pu, which is a significant change form the initial operation condition and the power flow in AC and DC transmission line from bus 16 to bus 17 are heavy, approximately 171 MW and 100 MW. A single three-phase-ground fault is applied on the line 12-11 near bus 11 at $t = 1$ s, followed by switching off the faulty transmission line 12-11 at $t = 1.1$ s and reclose it $t = 1.9$ s. At $t = 2$ s, communication channel 1 and 2 failed.

Fig. 15 shows active response of the power transmission lines. As is shown in Fig. 15(a), the control performance of CWADC is worse than RWADC. The reason is that the operation condition is changed significantly but CWADC is a linear controller based on a specific operation condition. Moreover, with one or two communication failures, RWADC can still maintain a good control performance. According to Fig. 15(b), it can be found that when communication channels 1 and 2 fail, the system cannot suppress the oscillations without FLM. However, with FLM, the control performance of RWADC gets better gradually. Therefore, RWADC with FLM has a strong ability of adaptability, and it maintains a good control performance even with two channel communication failures.

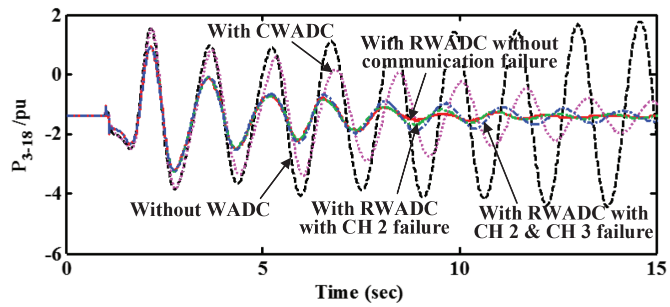

(a) Response of P_{3-18}.

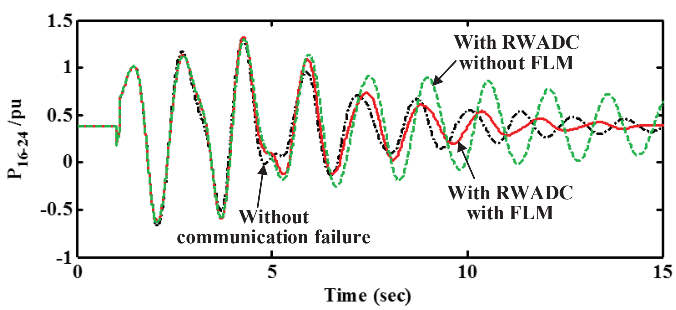

(b) Response of P_{16-24} (with CH 1 and CH 2 failure).

Fig. 15. Active power response of transmission lines (short circuit fault occurred on the line 12-11 near bus 11 at 1 s).

F. Communication Delay Existing in Wide-Area Signals

In this subsection, the impact of the communication delay existing in wide-area signal is considered. Fig. 16 shows the active response of the power transmission lines under CH2 and CH3 communication failure and 500ms time delay existing in wide-area signals. In this scenario, the adaptive delay compensator (ADC) proposed in our previous work [25] is added. As shown in Fig. 16, the proposed resilient WADC with ADC can handle the problem of communication failure and time delay at the same time and achieve a good damping performance. It is worth mentioning that proposed resilient WADC with ADC can compensate the both forward and feedback time delays effectively, as the effectiveness of the ADC in compensating the both constant and random delay has been fully verified in [25]. The related simulation results are omitted here due to the page limit.

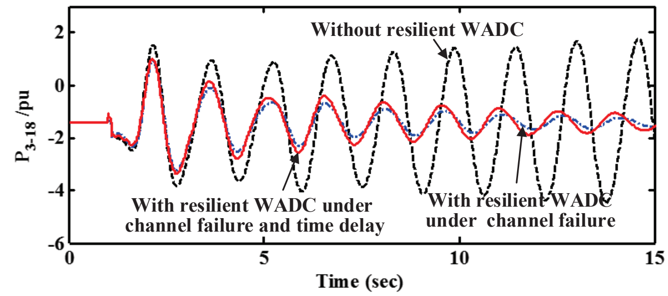

Fig. 16. Active power response of transmission line 3-18 under communication failure and time delay at the . (short circuit fault occurred on the line 12-11 near bus 11 at 1 s).

VI. Conclusions

To deal with the communication failure in wide-area control for interarea oscillations, this paper proposes a GrHDP and FLM based resilient WADC for the VSC-HVDC, which modulates the DC transmission power to damp interarea oscillation in an AC/DC power system. Simulation studies are conducted in a 10-machine 39-bus power system with one VSC-HVDC transmission line. Any one or two channel communication failures are both tested in this paper. Using three wide-area signals as input signals, the proposed resilient WADC can maintain a good damping performance under one or two channel communication failures. Simulation results also show the proposed resilient WADC has the advantages of online learning and strong adaptivity to realize a better damping performance than the conventional lead-lag WADC when operation conditions change a lot. The effectiveness of FLM is also tested and simulation results show that FLM can greatly increase the learning rate of GrHDP and enhance the regulation ability of the resilient WADC when encountering severe communication failures. In a word, the GrHDP and FLM based resilient WADC can achieve a satisfactory damping performance even though operation conditions vary significantly or severe communication failures occur. In addition, the resilient WADC can also applied for other equipment in the power system such as, excitation system of the synchronous generator, flexible AC transmission systems, and renewable generators. Future work will focus on designing resilient WADC for multiple critical weak interarea oscillations to tolerate communication failure.

References

[1] Y. Li, Y. Zhou, F. Liu, Y. J. Cao, and C. Rehtanz, "Design and implementation of delay-dependent wide-area damping control for stability enhancement of power systems," *IEEE Trans. Smart Grid*, vol. 8, no.4, pp. 1831-1842, Jul. 2017.

[2] W. Yao, L. Jiang, J. K. Fang, J. Y. Wen, S. J. Cheng, and Q. H. Wu, "Adaptive power oscillation damping controller of superconducting magnetic energy storage device for interarea oscillations in power system," *Int. J. Electr. Power Energy Syst.*, vol. 78, pp. 555-562, Jun. 2016.

[3] J. K. Fang, W. Yao, Z. Chen, J. Y. Wen, and S. J. Cheng, "Design of anti-windup compensator for energy storage-based damping controller to enhance power system stability," *IEEE Trans. Power Syst.*, vol. 29, no. 3, pp. 1175-1185, May 2014.
[4] W. Yao, L. Jiang, J. Y. Wen, Q. H. Wu, and S. Cheng, "Wide-area damping controller for power system interarea oscillations: A networked predictive control approach," *IEEE Trans. Control Syst. Technol.*, vol. 23, no. 1, pp. 27-36, Jan. 2015.
[5] Y. J. Cao, X. Y. Shi, Y. Li, Y. Tan, M. Shahidehpour, and S. L. Shi, "A simplified co-simulation model to investigate impacts of cyber-contingency on power system," *IEEE Trans. Smart Grid*, 2017, in press.
[6] W. Yao, L. Jiang, Q. H. Wu, J. Y. Wen, and S. J. Cheng, "Delay-dependent stability analysis of the power system with a wide-area damping controller embedded," *IEEE Trans. Power Syst.*, vol. 26, no.1, pp. 233-240, Jan. 2011.
[7] X. R. Zhang, C. Lu, S. C. Liu, and X. Y. Wang, "A review on wide-area damping control to restrain inter-area low frequency oscillation for large-scale power systems with increasing renewable generation," *Renewable Sustainable Energy Rev.*, vol. 57, pp. 45-48, May 2016.
[8] W. Yao, L. Jiang, J. K. Fang, J. Y. Wen, and S. R. Wang, "Damping of inter-area low frequency oscillation using an adaptive wide-area damping controller," *J. Electr. Eng. Technol.*, vol. 9, no. 1, pp. 27-36, Jan. 2014.
[9] S. Zhang and V. Vittal, "Design of wide-area power system damping controllers resilient to communication failures," *IEEE Trans. Power Syst.*, vol. 28, no. 4, pp. 4292-4300, Nov. 2013.
[10] F. R. S. Sevilla, I. Jaimoukha, B. Chaudhuri, and P. Korba, "Fault-tolerant wide-area control for power oscillation damping," in *Proc. IEEE PES Gen. Meeting Conf.*, Jul. 2012, pp. 1-8.
[11] S. Zhang and V. Vittal, "Wide-area control resiliency using redundant communication paths," *IEEE Trans. Power Syst.*, vol. 29, no.5, pp. 2189-2199, Sept. 2014.
[12] M. E. Raoufat, K. Tomsovic, and S. M. Djouadi, "Virtual actuators for wide-Area damping control of power systems," *IEEE Trans. Power Syst.*, vol. 31, no. 6, pp. 4703-4711, Nov. 2016.
[13] J. J. Duan, H. Xu, and W. X. Liu, "Q-learning based damping control of wide-area power systems under cyber uncertainties," *IEEE Trans. Smart Grid*, 2017, in press.
[14] M. Bhadu, N. Senroy, I. N. Kar, and G. N. Sudha, "Robust linear quadratic Gaussian-based discrete mode wide area power system damping controller," *IET Gener. Transm. Distrib.*, vol. 10, no.6, pp. 1470-1478, Apr. 2016.
[15] S. Khosravani, I. N. Moghaddam, and A. Afshar, M. Karrari, "Wide-area measurement-based fault tolerant control of power system during sensor failure," *Electr. Power Syst. Res.*, vol. 137, pp. 66-75, Nov. 2016.
[16] C. Lu, J. Si, and X. Xie, "Direct heuristic dynamic programming for damping oscillations in a large power system," *IEEE Trans. Syst. Man Cybern. Part B Cybern.*, vol. 38, no. 4, pp. 1008-1013, Aug. 2008.
[17] J. Si, A. G. Barto, W. B. Powell, and D. C. Wunsch, Eds., *Handbook of Learning and Approximate Dynamic Programming*. New York, NY, USA: IEEE Press, 2004
[18] S. Ray, G. K. Venayagamoorthy, B. Chaudhuri, and R. Majumder, "Comparison of adaptive critic-based and classical wide-area controllers for power systems," *IEEE Trans. Syst., Man, Cybern. B, Cybern.*, vol. 38, no. 4, pp. 1002-1007, Aug. 2008.
[19] D. Molina, G. Venayagamoorthy, J. Liang, and R. Harley, "Intelligent local area signals based damping of power system oscillations using virtual generators and approximate dynamic programming," *IEEE Trans. Smart Grid*, vol. 4, no. 1, pp. 498-508, Mar. 2013
[20] H. B. He, Z. Ni, and F. Jian, "A three-network architecture for on-line learning and optimization based on adaptive dynamic programming," *Neurocomputing*, vol. 78, no. 1, pp. 3-13, Jan. 2012.
[21] X. N. Zhong, Z. Ni, and H. B. He,"A theoretical foundation of goal representation heuristic dynamic programming," *IEEE Trans. Neural Networks Learn. Syst.*, vol. 27, no. 12, pp. 2513-2525, Dec. 2016.
[22] Y. F. Tang, H. B. He, Z. Ni, J. Y. Wen, and X. S. Chao, "Reactive power control of grid-connected wind farm based on adaptive dynamic programming," *Neurocomputing*, vol. 125, pp. 125-133, Feb. 2014.
[23] X. C. Sui, Y. F. Tang, H. B. He, and J. Y. Wen, "Energy storage based low frequency oscillation damping control using particle swarm optimization and heuristic dynamic programming," *IEEE Trans. Power Syst.*, vol. 29, no. 5, pp. 2539-2548, Sept. 2014.
[24] Z. Ni, Y. F. Tang, X. Sui, H. B. He, and J. Y. Wen, "An adaptive neuro-control approach for multi-machine power systems," *Int. J. Electr. Power Energy Syst.*, vol. 75, pp. 108-116, Feb. 2016.
[25] Y. Shen, W. Yao, J. Y. Wen, and H. B. He, "Adaptive wide-area power oscillation damper design for photovoltaic plant considering delay compensation," *IET Gener. Transm. Distrib.*, vol. 11, no. 18, pp. 4511-4519, Dec. 2017.
[26] L. Jiang, W. Yao, J. Y. Wen, Q. H. Wu, and S. J. Cheng, "Delay-dependent stability for load frequency control with constant and time-varying delays," *IEEE Trans. Power Syst.*, vol. 27, no. 2, pp. 932-941, May 2012.
[27] A. Fuchs, M. Imhof, T. Demiray, and M. Morari, "Stabilization of large power systems using VSC-HVDC and model predictive control," *IEEE Trans. Power Delivery*, vol. 29, no. 1, pp. 480-488, Feb. 2014.
[28] Y. Pipelzadeh, B. Chaudhuri, and T. C. Green, "Control coordination within a VSC-HVDC link for power oscillation damping: a robust decentralized approach using homotopy," *IEEE Trans. Control Syst. Technol.*, vol. 21, no. 4, pp. 1270-1279, Jul. 2013.
[29] Y. F. Tang, H. B. He, Z. Ni, J. Y. Wen, and T. W. Huang, "Adaptive modulation for DFIG and STATCOM with high-voltage direct current transmission," *IEEE Trans. Neural Networks Learn. Syst.*, vol. 27, no. 8, pp. 1762-1772, Aug. 2016.
[30] Y. Shen, W. Yao, J. Y. Wen, H. B. He, and W. B. Chen, "Adaptive supplementary damping control of VSC-HVDC for interarea oscillation using GrHDP," *IEEE Trans. Power Syst.*, 2017, in press.
[31] S. Cole, J. Beerten, and R. Belmans, "Generalized dynamic VSC MTDC model for power system stability studies," *IEEE Trans. Power Syst.*, vol. 25, no. 3, pp. 1655-1662, Aug. 2010.
[32] M. Mokhtari, F. Aminifar, D. Nazarpour, and S. Golshannavaz,"Wide-area power oscillation damping with a fuzzy controller compensating the continuous communication delays,"*IEEE Trans. Power Syst.*, vol. 28, no.2, pp. 1997-2005, May 2013.
[33] W. Yao, L. Jiang, J. Y. Wen, Q. H. Wu, and S. J. Cheng, "Wide-area damping controller of FACTS devices for inter-area oscillations considering communication time delays," *IEEE Trans. Power Syst.*, vol. 29, no.1, pp. 318-329, Jan. 2014.
[34] C. Canizares, T. Fernandes, E. G. Junior, G. L. Luc, M. Gibbard, I. Hiskens, J. Kersulis, R. Kuiava, L.Lima, F. D. Marco, N.Martins, B. C. Pal, A. Piardi, R. Ramos, J. dos Santos; D. Silva, A. K. Singh, B. Tamimi, and D. Vowles, "Benchmark models for the analysis and control of small-signal oscillatory dynamics in power systems," *IEEE Trans. Power Syst.*, vol. 32, no.1, pp. 715-722, Jan. 2017.
[35] Y. Zhang and A. Bose, "Design of wide-area damping controllers for interarea oscillations," *IEEE Trans. Power Syst.*, vol. 23, no.3, pp. 1136-1143, Aug. 2008.
[36] Y. Li, C. Rehtanz, S. Rüberg, L. F. Luo, and Y. J. Cao "Wide-area robust coordination approach of HVDC and FACTS Controllers for damping multiple interarea oscillations," *IEEE Trans. Power Delivery*, vol. 27, no.3, pp. 1096-1105, Jul. 2012.
[37] J. Liu, J. Y. Wen, W. Yao, and Y. Long, "Solution to short-term frequency response of wind farms by using energy storage systems," *IET Renewable Power Gener.*, vol. 10, no. 5, pp. 669-678, May 2016.

Yu Shen (S'17) received the B.S. degree in electrical engineering from Huazhong University of Science and Technology (HUST), Wuhan, China, in 2011 and 2015. Since September 2015, she has been pursuing the M.S. degree in the School of Electrical and Electronics Engineering, HUST, Wuhan, China. Her current research interests include power system stability analysis, adaptive dynamic programming, and optimal control.

Wei Yao (M'13-SM'17) received the B.S. and Ph.D. degrees in electrical engineering from Huazhong University of Science and Technology (HUST), Wuhan, China, in 2004 and 2010, respectively. He was a Post-Doctoral Researcher with the Department of Power Engineering, HUST, from 2010 to 2012 and a Postdoctoral Research Associate with the Department of Electrical Engineering and Electronics, University of Liverpool, Liverpool, U.K., from 2012 to 2014. Currently, he has been an Associate Professor with the School of Electrical and Electronics Engineering, HUST, Wuhan, China. His current research interests include power system stability analysis and control, HVDC & FACTS, and renewable energy.

Jinyu Wen (M'10) received the B.S. and Ph.D. degrees in electrical engineering from Huazhong University of Science and Technology (HUST), Wuhan, China, in 1992 and 1998, respectively.

He was a Visiting Student from 1996 to 1997 and Research Fellow from 2002 to 2003 all at the University of Liverpool, Liverpool, UK, and a Senior Visiting Researcher at the University of Texas at Arlington, Arlington, USA, in 2010. From 1998 to 2002 he was a Director Engineer with XJ Electric Co. Ltd. in China. In 2003, he joined the HUST and now is a Professor with the School of Electrical and Electronics Engineering, HUST. His current research interests include renewable energy integration, energy storage, multi-terminal HVDC and power system operation and control.

Haibo He (F'17) received the B.S. and M.S. degrees in electrical engineering from Huazhong University of Science and Technology, China, in 1999 and 2002, respectively, and the Ph.D. degree in electrical engineering from Ohio University in 2006. From 2006 to 2009, he was an Assistant Professor at the Department of Electrical and Computer Engineering at Stevens Institute of Technology. Currently, he is the Robert Haas Endowed Chair Professor at the Department of Electrical, Computer, and Biomedical Engineering at the University of Rhode Island. His research interests include adaptive dynamic programming, computational intelligence, machine learning and data mining, and various applications. He has published 1 sole-author research book (Wiley), edited 1 book (Wiley-IEEE) and 6 conference proceedings (Springer), and authored and co-authored over 250 peer-reviewed journal and conference papers. He severed as the General Chair of the IEEE Symposium Series on Computational Intelligence (SSCI 2014). He was a recipient of the IEEE International Conference on Communications Best Paper Award (2014), IEEE Computational Intelligence Society (CIS) Outstanding Early Career Award (2014), National Science Foundation (NSF) CAREER Award (2011), and Providence Business News (PBN) Rising Star Innovator Award (2011). Currently, he is the Editor-in-Chief of the IEEE Transactions on Neural Networks and Learning Systems.

L. Jiang (M'00) received the B.Sc. and M.Sc. degrees from Huazhong University of Science and Technology (HUST), Wuhan, China in 1992 and 1996, respectively, and the Ph.D. degree from the University of Liverpool, Liverpool, U.K., in 2001, all in electrical engineering.

He was a Postdoctoral Research Assistant with The University of Liverpool, Liverpool, U.K., from 2001 to 2003 and a Postdoctoral Research Associate with the Department of Automatic Control and Systems Engineering, University of Sheffield, Sheffield, U.K., from 2003 to 2005. He was a Senior Lecturer with the University of Glamorgan from 2005 to 2007 and joined the University of Liverpool in 2007. Currently, he is a Reader with the Department of Electrical Engineering and Electronics, The University of Liverpool. His current research interests include control and analysis of power system, smart grid, and renewable energy.